UCRL--94164-Rev.2

DE87 001363

UCRL- 94164 REV. 2
PREPRINT

THE APPLICATION OF ATOMIC VAPOR LASER ISOTOPE SEPARATION TO THE ENRICHMENT OF MERCURY

J. CRANE, G. ERBERT
J. PAISNER, H. CHEN
Z. CHIBA, R. BEELER
R. COMBS, S. MOSTEK

THIS PAPER WAS PREPARED FOR SUBMITTAL TO

THIRD INTERNATIONAL SYMPOSIUM ON RESONANCE IONIZATION SPECTROSCOPY AND ITS APPLICATIONS
SWANSEA, WALES
SEPTEMBER 7-12, 1986

SEPTEMBER 1986

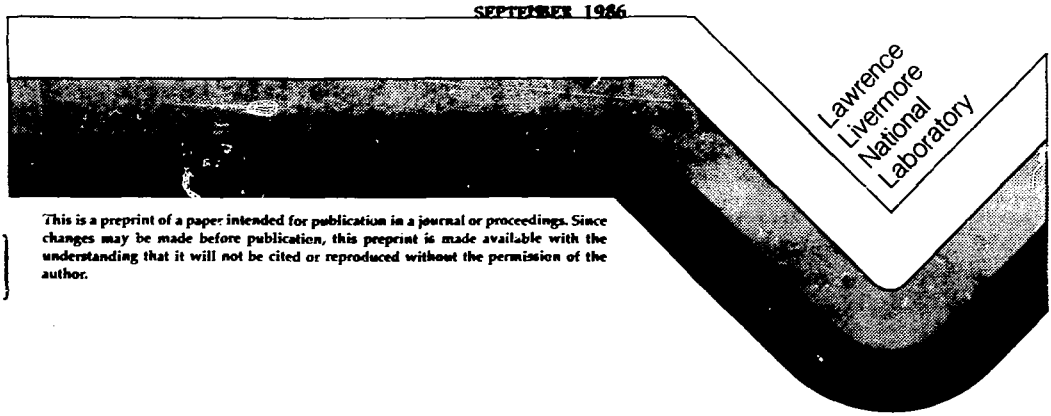

THE APPLICATION OF ATOMIC VAPOR LASER ISOTOPE SEPARATION TO THE ENRICHMENT OF MERCURY *

ABSTRACT

Workers at GTE/Sylvania have shown that the efficiency of fluorescent lighting may be markedly improved using mercury that has been enriched in the ^{196}Hg isotope. A 5% improvement in the efficiency of fluorescent lighting in the United States could provide a savings of $450 million dollars in the corresponding reduction of electrical power consumption. We discuss the results of recent work done at our laboratory to develop a process for enriching mercury. The discussion centers around the results of spectroscopic measurements of excited-state lifetimes, photoionization cross sections, and isotope shifts.

1. Introduction

Atomic vapor laser isotope separation (AVLIS) is a useful and economically attractive technique for the large-scale enrichment of uranium. In addition to uranium, for which the demand is greater than 1000 metric tons per year, there are smaller-scale applications for several other isotopically enriched elements. Researchers at GTE/Sylvania (Maya et al., 1984) have shown that the efficiency of standard fluorescent lamps used for lighting may be improved by approximately 5% by using mercury that has been enriched in isotope 196. The primary radiation source in a fluorescent lamp is emission from the electronically excited 6^3P_1 state to the ground state. This emission at 2537 Å is strongly trapped on the other mercury isotopes (198, 199, 200, 201, 202, and 204) that comprise from 6.8% for ^{204}Hg to 29.3% for ^{202}Hg in natural mercury. Natural mercury contains only .15% of ^{196}Hg and, as a result, does not trap radiation at 2537 Å emitted from these atoms at the operating densities of a fluorescent lamp. By increasing the portion of ^{196}Hg up to 3%, an additional channel for untrapped radiation is available, providing an overall increase in lamp emission and efficiency of ~5%. Enriching the mercury beyond this point provides little additional improvement due to an

*This work was performed under the auspices of the U.S. Department of Energy by Lawrence Livermore National Laboratory under contract No. W-7405 - Eng.48.

increase in resonant energy transfer among isotopes. The motivation for providing isotopically enriched mercury is to provide more efficient lighting. Since the United States consumes 1.8×10^{11} kWh at 0.05$/kWh annually in powering fluorescent lamps, a 5% increase in efficiency would yield a savings of $450 million annually.

2. Isotope-Selective Ionization of Mercury

The design of an AVLIS process in any element inevitably centers around the ionization and associated atomic physics. The photoionization of mercury represents a departure from most of the schemes we have studied for the lanthanides and other transition elements. At 10.4 eV, the ionization potential (IP) of mercury is several volts higher than the IP of the lanthanides or actinides. With mercury's filled shells and relatively simple electronic configuration, there are fewer levels and consequently fewer choices for a suitable photoionization ladder. Absorption spectroscopy measurements dating back to the 1930s reveal autoionizing levels above the $5d^{10}6S$ ei continua that belong to Rydberg series converging to the lowest excited ion states at 35,514 cm^{-1}, 50,552 cm^{-1}, and 51,488 cm^{-1}.

Dyer (1985) photoionized mercury in three resonant steps to the $5d^9 6s^2 6p$ ($^3P_1$) autoionizing level where 6^3P_1 and 8^1S_0 were the intermediate levels. We have excited mercury to this state using three-step ladders that first pump mercury to the 6^3P_1 state, then to one of the following levels: 6^3D_1, 6^3D_2, 7^3D_1, 7^3D_2, 7^1D_2, 8^1S_0, or 8^3S_1. The final step pumps mercury to the autoionizing level $5d^9 6s^2 6p(^3P_1)$ at 88,760 cm^{-1}. Figure 1 shows data for the relative photoionization cross section vs energy above the ground state where the upper state of the second step in our ladder is 6^3D_2. The relative cross section is given by:

$$\sigma_R = \frac{S_i}{E \cdot S_f} ,$$

where S_i is the ion signal, S_f is the fluorescence signal from the 6^3D_2 state, and E is the third-step laser fluence. The curve is a composite of curves covering seven different dyes for the third-step

laser. The position of the autoionizing level given in Moore (1971) is shown and the line width is comparable to the value 1653 cm^{-1} measured by Cairns (1970). Unfortunately, the peak photoionization cross section of the $5d^{10}6s6d(6^3D_2) \rightarrow 5d^9 6s^2 6p(^3P_1)$ transition does not appear to be substantially larger than the cross section for photoionization to the continuum.

Another candidate for resonant photoionization in mercury would be a two-step scheme: $5d^{10}6s^2\ (6^1S_0) \rightarrow 5d^{10}6s6p\ (6^3P_1) \rightarrow 5d^{10}6p^2\ (6^3P'_0)$. We generate the two ultraviolet transitions by Raman shifting in H_2 the output of our YAG-pumped dye lasers. For the first step transition at 2537 Å, we take the first anti-Stokes order of the frequency-doubled dye-laser output at 5673 Å. For the transition to the autoionizing level at 1974 Å, we take the eighth anti-Stokes order of the dye-laser output at 5733 Å. The lower trace in Fig. 2 shows ion signal vs second-step laser frequency, revealing a strong resonance. The upper trace in this figure is the signal from the pyroelectric detector used to measure laser energy. The dips in laser energy that produce corresponding decreases in ion signal are due to the $v'' = 0 \rightarrow v' = 2$ Schumann-Runge absorption band in O_2. Our measured value of 90,099 cm^{-1} for the $6p^2\ (6^3P'_0)$ level differs from the previous listing of 90,096 cm^{-1} for this level (Moore, 1971).

To determine the photoionization cross section for the transition $5d^{10}6s6p\ (6^3P_1) \rightarrow 5d^{10}6p^2\ (6^3P'_0)$, we measured ion signal vs laser fluence and fit the resulting saturation curve to a rate-equation model. The value we have measured for the peak photoionization cross section for this transition is $3 \pm 2 \times 10^{-15}$ cm^2. To fully illuminate a large cross-sectional area of vapor in a mercury separator, we would need several watts of average power at 1974 Å for this two-step photoionization scheme. We are investigating methods for generating this coherent UV radiation.

An alternative to resonant photoionization to an autoionizing level is photoionization to the continuum. The threshold photoionization cross

section to the continuum increases as a function of principal quantum number. One clearly obtains an advantage by first exciting the atom to a high-lying state, then photoionizing to just above the threshold. A slight variation of this concept would be to choose an efficient high-average-power IR laser for photoionization, then excite the atom to the lowest level from which the atom can be photoionized.

We have designed a mercury enrichment process based on a three-step photoionization ladder using a 1.06-μm solid-state laser for the final transition to the continuum from one of three 7d states. In the remainder of this talk, we will discuss the existing data base for this particular photoionization scheme.

We have measured radiative lifetimes for the 7^1D_2, 7^3D_1, and 7^3D_2 states using two-step laser-induced fluorescence. These measurements have been made in a low-pressure static cell. We send two laser pulses, the first tuned to the $6^1S_0 \rightarrow 6^3P_1$ transition and the second tuned from 6^3P_1 to one of the three accessible states of the $5d^{10}6s7d$ configuration. We detect fluorescence from the excited state with an RCAC31034 photomultiplier tube and a fast transient digitizer. Figure 3 shows results for these measurements along with values reported by other authors. We have also used this technique for measuring the radiative lifetime of the 6^3P_1 state, corroborating a value of ~120 ns measured by several authors (Halstead et al., 1982 and King et al., 1974).

We have measured the photoionization cross section for the 1.06-μm radiation for each of the three 7d states using the saturation technique described earlier. Figure 4 shows a plot of ion signal vs 1.06-μm laser fluence. From this measurement we obtain a value of $1.35 \pm 0.21 \times 10^{-17}$ cm^2 for the photoionization cross section of the 7^3D_1 state using 1.06-μm photons.

Measurements of the hyperfine structure and isotope shifts of the first step, 6^1S_0 to 6^3P_1, have been made by numerous authors including ourselves (Crane, 1985). Gerstenkorn (1977) gives values for the isotope shifts for the 6^3P_1 to 7d states that we use in our photoionization

data base. Finally, using the measured values for cross sections, radiative lifetimes, oscillator strengths, etc. that we have compiled in our photoionization data base, we can model photo-ionization vs laser fluence by integrating the density matrix equations relevant to our atomic system. Based on these predictions we are currently working on the design for a laser system for enriching mercury.

References

Anderson T, Sorensen G 1973 J. Quant Spectrosc Rad Transfer 13 269

Cairns R B, Harrison H, Schoen R I 1970 J. Chem Phys 53 96

Crane J K, Erbert G V, Mostek S D, Kerlin R C, Paisner J A 1985 Proc. 1st Intl Laser Conf.

Dyer P, Baldwin G C, Sabbas A M, Kittrell C, Schweitzer E L, Abramson E, Imre D G 1985 J. Appl Phys 58 2431

Faisal F H M, Wallenstein R, Teets R 1980 J. Phys B 13 2077

Gerstenkorn S, Labarthe J J, Verges J 1977 Physica Scripta 15 167

Halstead J A, Reeves R R, 1982 J. Quant Spectrosc. Radiat. Transfer 28 289

King G C, Adams A 1974 J. Phys B 7 1712

Maya J, Grossman M W, Lagushenko R, Waymouth J F 1984 Science 226 435

Moore C E, 1971 Atomic Energy Levels, NBS 35 3 195

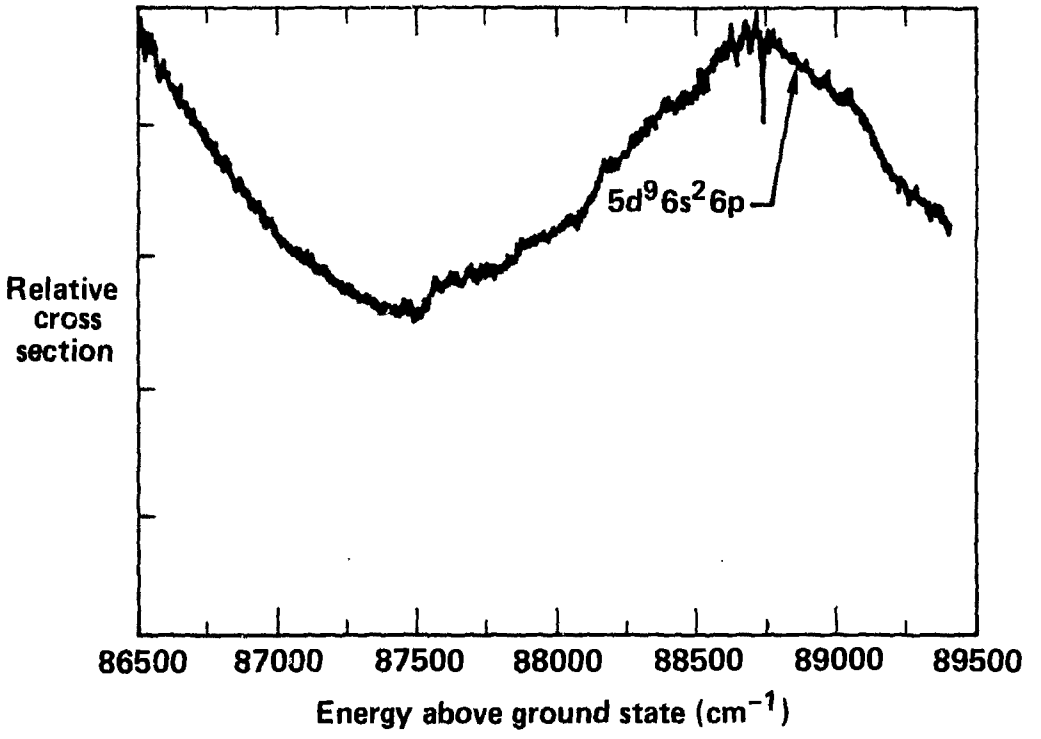

Fig. 1. Relative photoionization cross section vs energy for photoionization from the 6^3D_2 state.

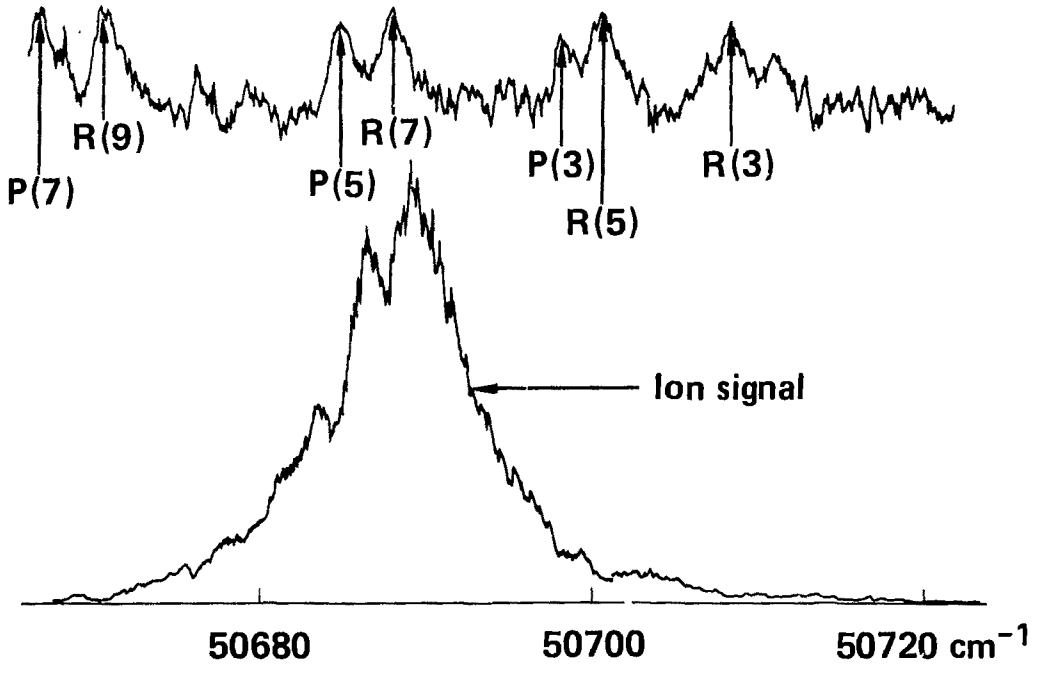

Fig. 2. Mercury autoionizing transition: $5d^{10}6s6p(6^3P_1) \rightarrow 5d^{10}6p^2\ (6^3P'_0)$; upper trace, laser intensity, shows absorption band in O_2: $X^3\Sigma g^- \rightarrow B^3\Sigma u\tau v'' = 0 \rightarrow v' = 2$.

30-90-0586-6225

STATE	LIFETIME (ns)	
	This work	Others
7^1D_2	41.5 ± 2.6	40.0 ± 1.0[a]
7^3D_1	13.4 ± 0.6	14 ± 3[b]
7^3D_2	17.5 ± 0.8	

a. FHM Faisal, R. Wallenstein, R. Teets, J. Phys. B 13, 2077 (1980)
b. T. Anderson, G. Sorensen, J. Quant. Spectrosc. Rad. Transfer 13, 269 (1973)

Fig. 3. Excited-state lifetime measurements in mercury using laser-induced fluorescence.

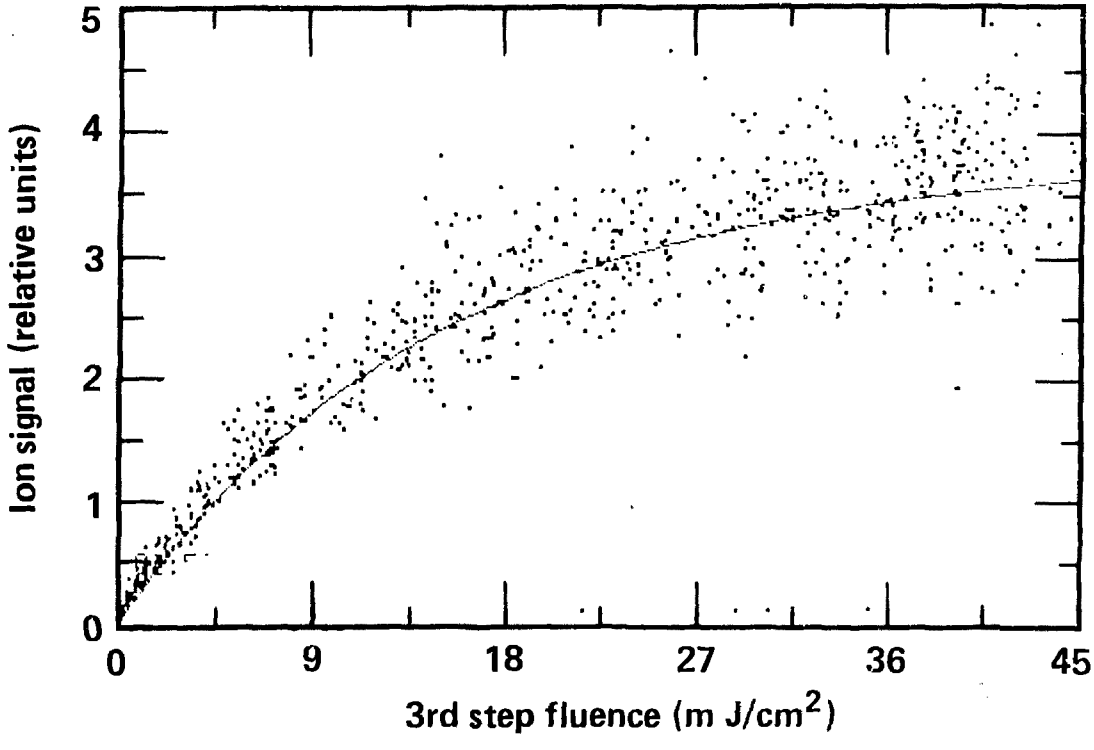

Fig. 4. Typical data of photoion signal vs third-step fluence for $7^3D_1 \rightarrow$ continuum at 1.06 μm. Solid curve represents the nonlinear least-squares analysis.